Shape Adaptive Grinding (SAG): a new Process for Finishing of Ceramics and High-performance Alloys

Anthony BEAUCAMP[1], Atsushi MATSUBARA[1], Samyak JAIN[2], Christophe BOUVIER[2], and Roger MORTON[2]
[1] Department of Micro-Engineering, Kyoto University, Japan, beaucamp@me.kyoto-u.ac.jp
[2] Research and Development, Zeeko LTD, United Kingdom, christophe.bouvier@zeeko.co.uk

Abstract:
Shape Adaptive Grinding (SAG) is a new process for freeform finishing of difficult materials such as ceramics and high-performance alloys. The basic principle of SAG can be described as "semi-elasticity": compliance is achieved with freeform workpieces by an elastic spherical tool, while hard contact is simultaneously achieved by small rigid pellets covering this elastic tool (diamond or cubic boron nitride super-abrasives are embedded in these pellets). In this paper, we present recent developments in the application of SAG to (1) corrective grinding of aspheric silicon carbide optics, and (2) smoothing of high-performance titanium alloy components produced by additive manufacturing.

Keywords: Shape adaptive grinding, Ultra-precision, Finishing, Freeform, Ceramics, High-performance alloys

1. Introduction

The fabrication of complex shapes using materials such as ceramics or high-performance alloys, for temperature and corrosion resistant applications, usually relies on one of two methods that have become increasingly ubiquitous in industry: high-speed 5-axis machining (HSM), or more recently additive manufacturing (AM).

HSM can be used to machine complex shapes into alloys, but also graphite substrates [1]. These graphite substrates are then coated with a layer of silicon carbide by chemical vapor deposition (CVD) to produce a highly resistant surface [2]. Such components can be used for example in molding alumino-silicate glass under high temperature (above 800 °C). This allows manufacturing of curved scratch resistant screens for smartphones.

In the case of AM, electron beam melting (EBM) and selective laser sintering (SLS) [3] are cutting-edge processes used to produce three dimensional shapes by melting layers of metal powder. More specifically, in the case of EBM a dual scan of each layer is performed in a vacuum. The first scan serves as a pre-heat stage, and the second scan fully melts the powder. This procedure achieves more uniform part temperature during the process as compared to other AM techniques. The result is a fully dense part with a significant reduction in residual stresses. This translates to material properties that are superior to other AM methods and leads to its use in applications such as dental and prosthetic implants, or the prototyping of aeronautical components.

However, a limitation associated with both HSM and AM methods is the inability to produce highly finished surfaces (with surface roughness less than 50 nm Ra). In the case of HSM, the surface roughness is usually above 1 µm Ra, especially if the surface was subsequently coated with a CVD layer that results in a nodular surface texture, as shown in Fig. 1(a). As for AM, the typical surface finish on SLS and EBM surfaces is usually lumpy in appearance and the roughness in the order of several microns Ra, as shown in Fig. 1(b).

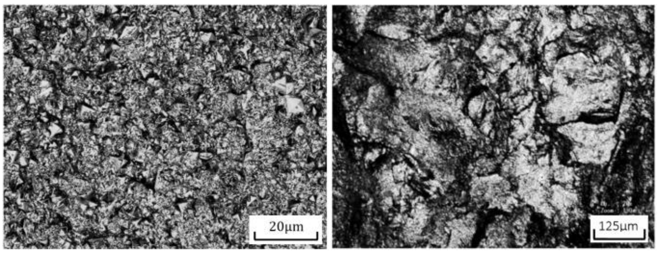

(a) CVD silicon carbide (b) AM titanium alloy

Figure 1: Confocal laser micrographs of raw surfaces.

Existing methods to improve surface roughness include traditional machining such as belt grinding or milling [4], chemical etching for porous structures [5], and re-melting by either laser polishing [6] or large area electron beam irradiation [7]. Reduction down to 2-3 µm Ra (from 22-45 µm Ra) was reported for additively manufactured titanium alloy parts using laser polishing. Other methods involving conformal grinding and polishing are sometimes applicable to complex additively manufactured shapes such as jet-engine blisks. But they usually only achieve roughness around 0.5 µm Ra [8].

Although each of the above finishing methods has a distinct advantage, such as being able to finish porous structures, the resulting surface roughness is still very high. Recently, we introduced a novel finishing process called Shape Adaptive Grinding (SAG), which we demonstrated to deliver ductile mode grinding on CVD silicon carbide [9]. In this paper, we demonstrate that iterative shape accuracy improvement using SAG is possible, by processing an aspheric optical mirror manufactured by HSM (then coated with a ceramic layer). We also report on progress towards implementing the SAG technology on low-cost machining centers. A Fanuc Robodrill was used to process an AM manufactured freeform workpiece by SAG (Ti-6Al-4V printed by SLS). Final surface roughness in the order of 10-20 nm Ra is demonstrated in both cases.

2. Shape Adaptive Grinding

The basic principle of SAG is illustrated in Fig. 2, and can be described as "semi-elasticity": using an elastic spherical tool, overall compliance is achieved with freeform workpieces over a sub-aperture grinding area, while hard contact is simultaneously achieved at relatively smaller scale thanks to rigid pellets covering the elastic tool. The deformability of the elastic layer allows the tool to conform to freeform surfaces featuring any convex curvature, or concave curvature larger than about twice the radius of the spherical SAG tool.

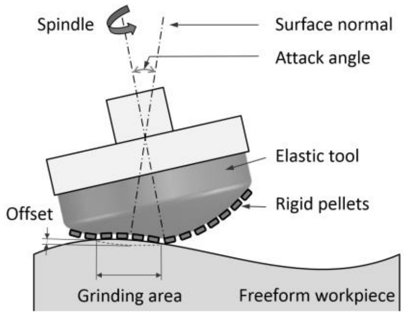

Figure 2: Principle of Shape Adaptive Grinding (SAG) [9].

Nickel or hard resin pellets are typically used, inside which super-abrasives such as diamond or cubic boron nitride (CBN) are embedded. The size of the grinding area is controlled by offsetting of the spherical tool against the workpiece, while the grinding direction and speed can be controlled independently through the angle of attack and rotation speed of the elastic spherical tool. This allows for control of the grinding spot in terms of contact area and removal rate. The elasticity of the tool can also be varied in order to control the grinding force. Finally, water or oil-based coolants can be used to clear debris.

3. Grinding of aspheric ceramic optic

3.1 Experimental parameters

A convex 90 mm diameter aspheric optical mirror (with deviation from best fit sphere of about 50 µm) was generated in industry by HSM. The surface was then coated with a 150 µm thick layer of silicon carbide by CVD. Using a contact profilometer, the form deviation of the component from its aspheric prescription was measured to be over 40 µm P-V. The average surface roughness was measured to be 4.3 µm Ra on a whitelight interferometer with 50x objective.

In order to improve both surface roughness and form deviation, the component was mounted inside a 7-axis Zeeko intelligent robotic polisher (IRP), as shown in Fig. 3. 20 mm radius SAG tools were used to grind the workpiece, with first 40 µm and then 9 µm diamonds, bonded in resin pellets.

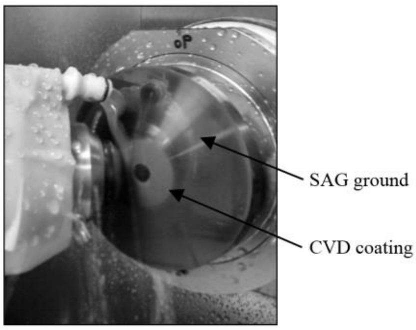

Figure 3: SAG machining of aspheric ceramic optic on Zeeko IRP machine.

In comparison with previous works, we wanted to demonstrate corrective capability. So in these experiments, the tool paths were programmed to moderate the surface feed of the grinding tool against the form deviation of the component (i.e: slower feeds at high points, faster at low points). The process parameters used in this experiment are summarized in Table 1.

Table 1: Process parameters

Machine parameters	
Tool path	Spiral
Track spacing	0.1 mm
Spindle speed	750 rpm
Attack angle	35 deg
Surface feed	10~1000 mm/min
Tool parameters	
Tool radius	20 mm
Tool offset	0.2 mm
Abrasives type	Diamonds in pellets
Abrasives size	40 and 9 um

3.2 Experimental results

The evolution of the surface roughness was monitored with the whitelight interferometer, as shown in Fig. 4. The CVD coating process produced a surface with grains of SiC grown to a nodular appearance (see Fig 4(a)). The 40 µm SAG tool was able to cut through these nodules, and leave a noticeably smoother surface (103 nm Ra).

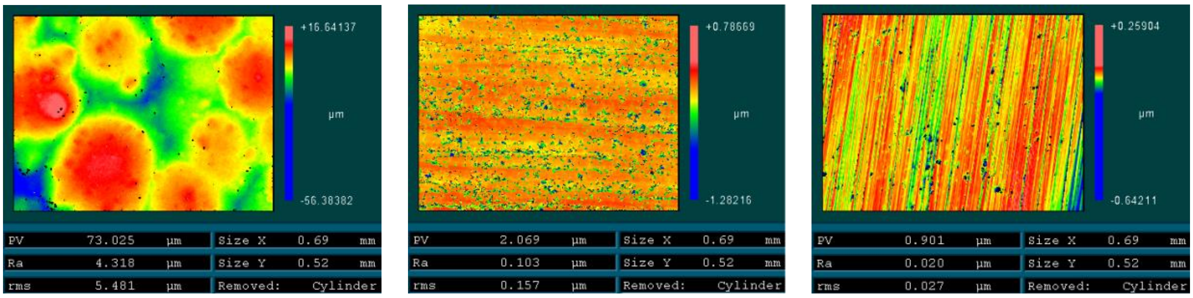

(a) As received (b) After SAG (40 µm diamond in resin) (c) After SAG (9 µm diamond in resin)

Figure 4: Evolution of surface texture on aspheric ceramic optic.

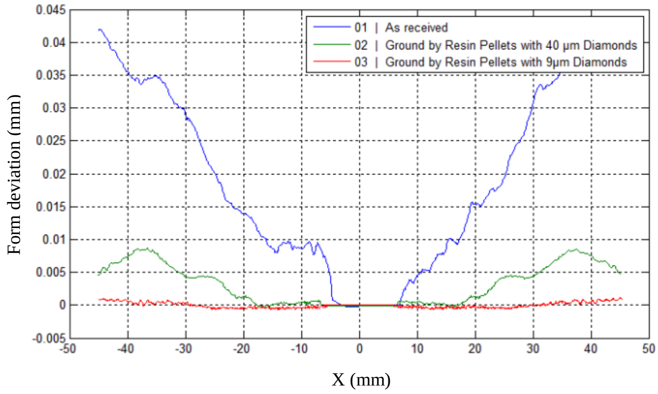

Figure 5: Evolution of aspheric form deviation.

Subsequent processing with the 9 µm SAG tool further reduced the surface roughness down to 20 nm Ra, with ductile/fracture mode grinding marks clearly visible on the measurement shown in Fig 4(c).

But importantly, through moderation of the surface feed of the SAG tools across the optical surface, it was simultaneously possible to iteratively improve the aspheric form deviation of the workpiece from over 40 µm P-V down to less than 2 µm P-V, as shown in Fig. 5. Processing by SAG improved the optical surface of the component sufficiently that the mirror could then be finished by ultra-precision deterministic polishing [10].

4. Grinding of AM titanium alloy workpiece

4.1 Experimental parameters

64 mm diameter freeform workpieces, designed to be representative of the range of geometries commonly encountered in medical implants (varying curvature, perforations on the main surface) were designed by 3D modelling and additively manufactured in industry by SLS of Ti-6Al-4V, as shown in Fig. 6.

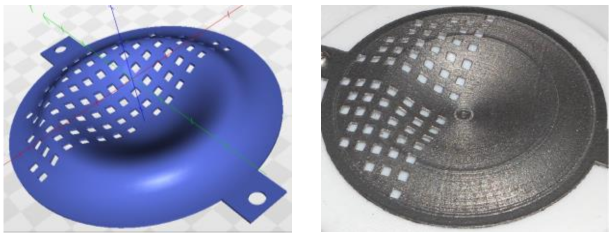

(a) 3D model of sample (b) 3D printed sample (SLS)

Figure 6: Additively manufactured titanium alloy sample.

SAG processing of the samples was then carried out on a 5-axis FANUC Robodrill machining center, using an optional rotary table attachment as shown in Fig. 7(a). In order to derive an estimate of the SAG tool geometry, a laser profiling unit was fitted on the machining center as shown in Fig 7(b). The spinning tool was plunged across the laser beam from various attack angles, in order to record the change in tool radius as a function of the attack angle. Fig. 8 shows a typical deviation curve, in which the tool radius varies across the range of attack angles and a depression is observed around 20-25 deg. This corresponds to the area used for grinding. This deviation curve can be updated between grinding runs, and used to compensate the geometrical position of the SAG tool against the surface.

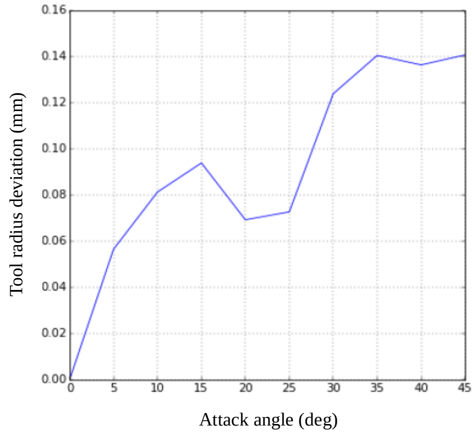

Figure 8: Tool radius deviation as function of attack angle.

Furthermore, because of the large tolerances (hundreds of microns) associated with additive manufacturing on the one-hand, and the large volumetric errors expected in the machining center on the other-hand, it was expected that a purely theoretical tool path would fail to grind the workpiece uniformly, since the SAG process is controlled using a geometric offset of only 300 microns.

To address this issue, a touch-trigger probe was fitted on the Robodrill as shown in Fig. 7(b). The probe was used to sense the location of the workpiece on-machine. Using a freeform data fitting algorithm the actual position and rotation (6-degrees of freedom) of the workpiece could be optimized. After optimization, residual form deviation of around 0.4 mm P-V was still left, as shown in Fig. 9.

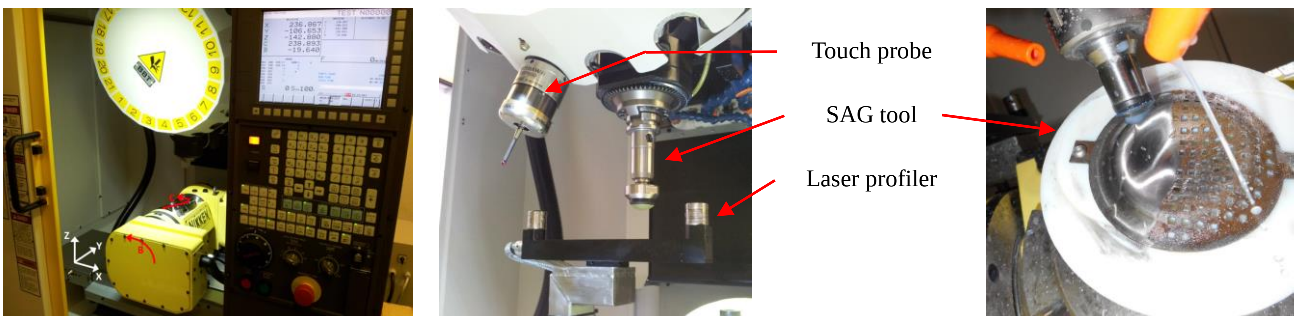

(a) 5-axis Robodrill machining centre (b) Tool and probe setup (c) SAG machining on Robodrill

Figure 7: SAG machining of AM titanium alloy component on 5-axis FANUC Robodrill.

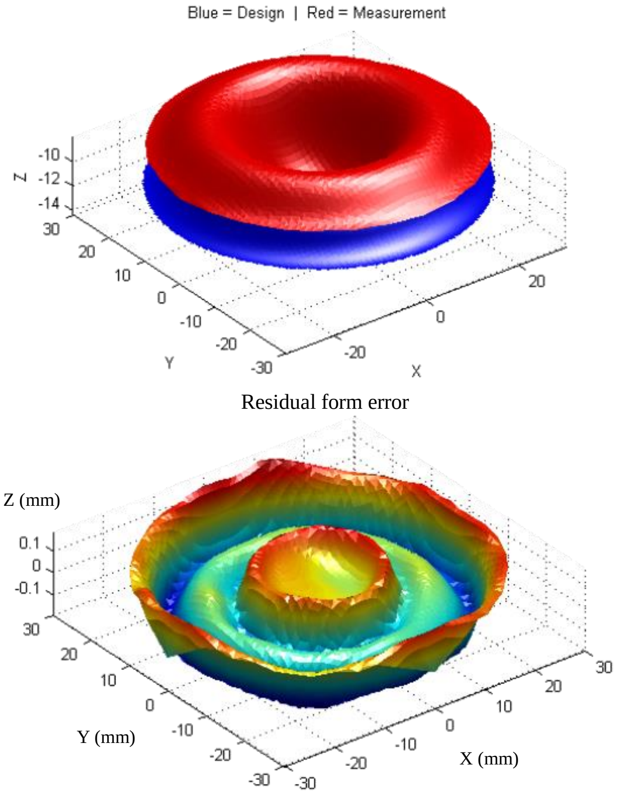

Figure 9: Residual shape deviation after freeform data fit.

This residual deviation map is the compound effect of large tolerances in additive manufacturing and the volumetric errors of the machine. But since it was measured on-machine, this map could be used directly to compensate the CNC path of the SAG tool across the workpiece.

To grind the AM workpieces, 10 mm radius SAG tools were employed, so that it was possible to reach inside the concave areas. 3 different types of pellets and abrasive sizes were used: Nickel bonded 40 µm, as well as Resin bonded 9 and 3 µm diamonds. The process parameters used for grinding the workpiece are summarized in Table 2. Raster tool paths were used to cover the workpiece surface.

Table 2: Process parameters

Machine parameters	
Tool path	Raster
Track spacing	0.15 mm
Spindle speed	750 rpm
Attack angle	20 deg
Surface feed	200 mm/min
Tool parameters	
Tool radius	10 mm
Tool offset	0.3 mm
Abrasives type	Diamonds in pellets
Abrasives size	40, 9, and 3 um

4.2 Experimental results

The surface of the first workpiece was sub-divided into quadrants, with a different level of processing targeted on each individual quadrant. Fig. 10 shows the cumulative processes for each of the four quadrants.

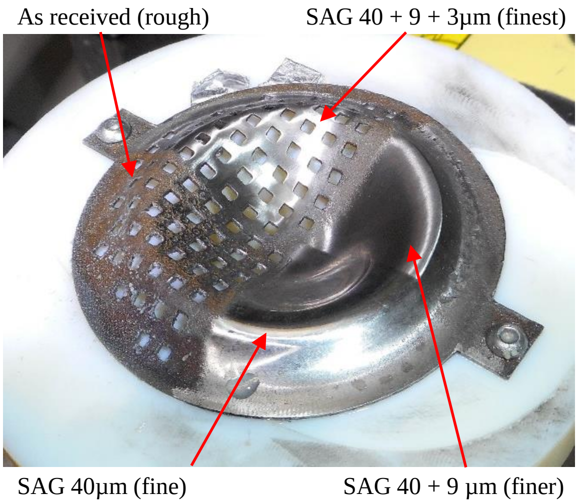

Figure 10: AM sample at various stages of SAG process.

The evolution of the surface roughness was monitored with a whitelight interferometer. The AM generated surface showed a lumpy appearance with roughness of 4.13 µm Ra. The 40 µm SAG tool was able to cut through these lumps, and leave a noticeably smoother surface (130 nm Ra). Subsequent processing further reduced the surface roughness, down to 65 nm Ra after the 9 µm SAG tool, and down to 8 nm Ra after the 3 µm SAG tool.

A second sample was processed, for which the entire surface was treated with the full series of SAG pellets: 40, 9 and 3 µm. The finished condition of the workpiece is shown in Fig. 11, which shows a mirror-like surface finish. The surface was characterized with a contact profilometer before and after processing, over a distance of 5mm (see Fig. 12). The surface roughness improved from 7.8 µm down to 18.0 nm Ra, an improvement of almost 3 orders of magnitude.

Figure 11: AM sample processed entirely by SAG.

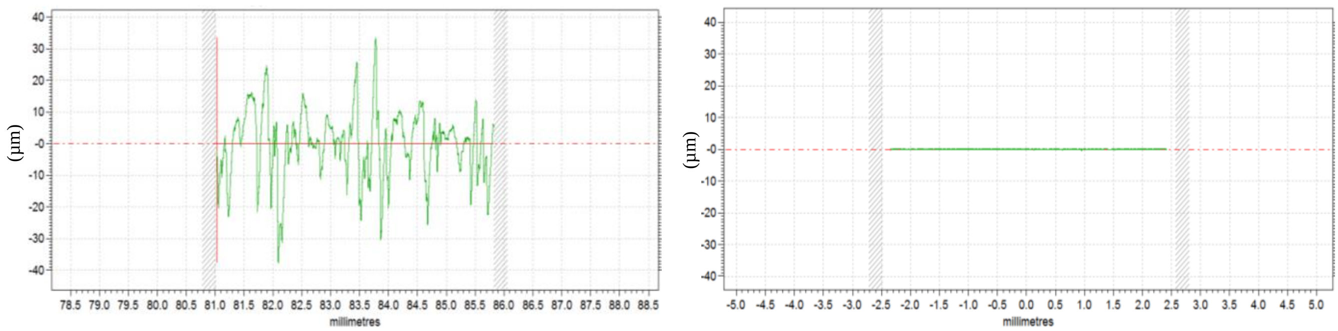

(a) As received (7.8 µm Ra)

(b) After 40, 9 and 3 µm SAG (18.0 nm Ra)

Figure 12: Evolution of surface texture on AM titanium alloy sample (same scale).

5. Conclusion

Shape Adaptive Grinding (SAG) is a novel process for freeform grinding of aspheric and freeform components, which has been applied to difficult materials such as ceramics and high-performance alloys.

Using the SAG process on a Zeeko polishing machine, it was possible to grind an aspheric ceramic optic. The surface roughness of the silicon carbide surface (produced by CVD coating method, which leaved a strongly nodular texture) was improved from 4.3 µm Ra down to 20 nm Ra using only two SAG tools with diamond abrasive sizes of 40 and 9 µm. Simultaneously, the form error was improved from over 40 µm P-V down to less than 2 µm P-V, through moderation of the tool feed across a spiral tool path. The resulting surface could then later be finished by ultra-precision polishing on the same machine.

It was also possible to use the SAG process on a 5-axis FANUC Robodrill machine, to grind an additively manufactured titanium alloy component. The roughness of an entire workpiece (produced by SLS method, which leaved a strongly lumpy texture) was improved from 7.8 µm Ra down to 18.0 nm Ra using three SAG tools with diamond abrasive sizes of 40, 9 and 3 µm.

It is important to note that these results were achieved using machines of very low stiffness, normally used in polishing and drilling (unlike the highly stiff and expensive machine tools normally used for precision grinding). The SAG method thus points towards a way to achieve lower costs in fine finishing of aspheric and freeform high-performance components.

References

[1] Schulz, H., and Moriwaki, T., 1992, High-speed machining, Annals of the CIRP, Vol. 41, No. 2, pp.637-643.

[2] Knowle, W., Withers, J., and Ronsone, P., 1995, CVD and CVR silicon based functionally gradient coating on carbon/carbon composite, Carbon, Vol. 33, No. 4, pp.415-426.

[3] Murr, L., Gaytan, S., Ramirez, D., Martinez, E., Hernandez J, and Amato, K, 2012, Metal fabrication by additive manufacturing using laser and electron beam melting technologies, Journal of Materials Science and Technology, Vol. 28, No. 1, pp.1-14.

[4] Narahara, H., Takeshita, S., Fukumaru, H., Koresawa, H., and Suzuki, H., 2012, Permeability performance on porous structure of injection mold fabricated by metal laser sintering combined with high speed milling, International Journal of Automation Technology, Vol. 6, No. 5, pp.576-583.

[5] Pyka, G., Burakowski, A., Kerckhofs, G., Moesen, M., Van Bael, S., and Schrooten, J., 2012, Surface modification of Ti6Al4V open porous structures produced by additive manufacturing, Advanced Engineering Materials, Vol. 14, No. 6, pp.363-370.

[6] Lamikiz, A., Sanchez, J., Lopez de Lacalle, L., and Arana, J., 2007, Laser polishing of parts built up by selective laser sintering, International Journal of Machine Tools & Manufacture, Vol. 47, pp.2040-2050.

[7] Uno, Y., Okada, A., Uemura, K., Raharjo, P., Furukawa, T., and Karato, K., 2005, High efficiency finishing process for metal mold by large-area electron beam irradiation, Precision Engineering, Vol. 29, pp.449–455.

[8] Duan, J., Shi, Y., Lin, X., and Dong, T., 2011, Flexible Polishing machine with dual grinding heads for aeroengine blade and blisk. Advanced Materials Research, Vol. 317, pp.2454-2460.

[9] Beaucamp, A., Namba, Y. , Combrinck, H. , Charlton, P., Freeman, R., 2014, Shape adaptive grinding of CVD silicon carbide, Annals of the CIRP, Vol. 63, No. 1, pp.317-320.

[10] Beaucamp, A., Namba, Y., Inasaki, I., and Freeman, R., 2011, Finishing of optical moulds to λ/20 by automated corrective polishing, Annals of the CIRP, Vol. 60, No. 1, pp.375-378.